

Reference Drag Update Scheme in Shuttle Entry Guidance Using Range Allocator for Tight Constraints

Erin Evans¹, Stephen Thrasher², and Jonathan P. How³

Abstract—Entry guidance with an improved drag profile update method is presented. The guidance method is a variation of Shuttle entry guidance in which the parameters that define the drag profile are modified to make the drag profile smooth and easier to customize. In general, in order to account for off-nominal entry conditions and ensure the vehicle flies the correct range, the nominal reference drag profile is modified online utilizing a first order approximation. This new profile is then used to calculate a reference drag command in the subsequent guidance algorithm cycle. Typical implementations of Shuttle entry guidance modify the drag profile using only one variable to shift the profile by a constant value. The methods by which the drag profile is updated are changed in order to provide multiple perturbation options. In providing multiple drag profile update parameters, an allocator is implemented with a vector of weights as a design variable. The resulting algorithm seeks to leverage the high-TRL Shuttle entry guidance routine by making minimal modifications to the implementation, while increasing robustness to dispersions under tight constraints. A discussion of drag profile design, including allocator parameter selection, is explored. Results for two highly constrained examples are presented, demonstrating the utility of this method.

I. INTRODUCTION

Shuttle guidance is the basis of many high L/D vehicle entry guidance methods. This entry guidance method is intended to provide steering commands from atmospheric entry to activation of the terminal area guidance about 50 nmi away from the runway. The algorithm uses a predetermined drag profile to define the trajectory, and modifies the profile for range control onboard by varying a small set of key parameters defining the profile. Trajectory reshaping via range control is necessary in order to capture and correct for modeling errors and uncertainties in vehicle aerodynamics and state at entry interface. However, it is important that range control be implemented in such a way that constraint margins are maximized where possible. The shuttle entry guidance method falls short when dealing with complex constraints that are easily violated when the drag profile is shifted by a constant value. This paper seeks to contribute a method that preserves the structure of the Shuttle heritage entry guidance methods, while satisfying complex constraints.

This paper focuses on the range control aspect of entry guidance, and contributes a method that is based on the

Shuttle entry guidance range control, which is outlined in detail in [1]. This method is unique in its simplicity and ability to leverage the high TRL shuttle algorithm by minimizing modifications to the original implementation. Previous range error update efforts include [2] in which the profile is scaled uniformly by a constant, and [3] - [4], in which the reference drag profile is scheduled on energy, resulting in more accurate range estimates for larger flight path angles and optimized with respect to heat load. [5] defines a reference profile using range to go among other states scheduled with energy, and implements an LQR controller to account for range error. [6] uses a set of trajectories computed offline, selecting a reference trajectory based on the current state, including range to the runway. This method guarantees convergence, but requires significant development time before each mission. Nonlinear programming is utilized to achieve a similar goal in [7]. Overall, these methods are more complex than the initial Shuttle entry guidance algorithm, both in implementation and in guarantees of convergence. The results are often not deterministic, and their performance can be hard to assess using Monte Carlo methods, which ultimately results in algorithms that are time consuming and difficult to validate for flight.

Shuttle guidance utilizes a predetermined drag profile and angle of attack profile scheduled on velocity. The angle of attack profile is typically designed to minimize heat rate, while the drag profile is designed to satisfy a number of constraints by remaining within the entry corridor while also flying a given range to the runway. These nominal profiles are designed to maximize constraint margin when plotted in drag-velocity space. The combination of these two profiles allows both bank angle magnitude and angle of attack to be determined, where bank angle modulation is the primary method of achieving the correct reference drag. There are typically four phases in a given drag profile. The first is the temperature control phase, delineated by a series of quadratic splines, the second is the pseudoequilibrium glide phase, which is also quadratic in velocity. The subsequent two phases are the constant drag phase and the transition phase, which is linear in energy.

This paper proposes a method for perturbing the reference drag profile that leverages the Shuttle algorithm structure while improving flexibility in order to satisfy more restrictive constraints. Within the capabilities of the Shuttle entry guidance algorithm, this method drastically increases the range of constraints that can be satisfied by a given vehicle.

The work outlined in this paper was developed with application to a vertical takeoff horizontal landing (VTHL)

¹Erin Evans is a graduate student in the Department of Aeronautics and Astronautics, Massachusetts Institute of Technology, 77 Massachusetts Ave., Cambridge, MA 02139, USA evanse@mit.edu

²Stephen Thrasher is a guidance engineer at Draper, 555 Technology Square, Cambridge MA 02139, USA sthrasher@draper.com

³Jonathan P. How is a professor in the Department of Aeronautics and Astronautics, Massachusetts Institute of Technology, 77 Massachusetts Ave., Cambridge, MA, 02139, USA jhow@mit.edu

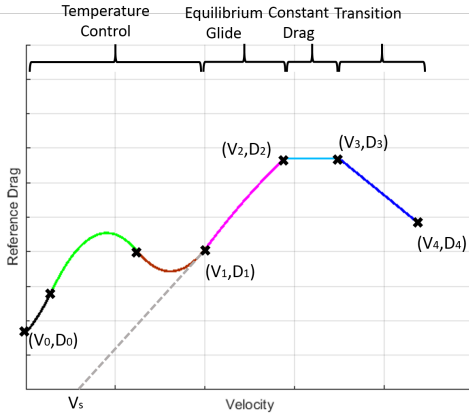


Fig. 1. Example reference drag profile with 4 phases: temperature control, equilibrium glide, constant drag, and transition, which are denoted at top of figure. Temperature control phase includes 4 knots to define three quadratic segments.

spaceplane in mind, and as a result the vehicle constraints and heating models used in this paper are based on such a vehicle using a high fidelity 6 DOF Reusable Launch Vehicle (RLV) simulation.

II. MOTIVATION

Entry guidance constraints are plotted in drag-velocity space in order to visualize the entry corridor through which the drag profile must be designed. The upper constraints are heat rate, acceleration, and dynamic pressure. When defining these constraints, L is lift, D is drag in an earth centered earth fixed coordinate frame, g is gravitational acceleration, V is vehicle velocity, and r is the distance between the vehicle and the origin of an earth centered coordinate frame.

The lower constraint is the minimum bank equilibrium glide condition, which occurs when the flight path angle, γ , is constant and crossrange control is absent,

$$L = g - \frac{V^2}{r} \quad (1)$$

Violating this constraint will cause the vehicle to exhibit phugoid motion, and eventually lose drag control authority. Given the angle of attack profile, this can be translated into a lower drag limit [8]:

$$D_{min} = \left(g - \frac{V^2}{r}\right) \left(\frac{L}{D}\right)^{-1} \quad (2)$$

A typical set of constraints are plotted in Figure 2, where multiple heat rate constraints for various points on the vehicle are all present. It should be noted that the velocity axis is decreasing in all relevant plots shown here. In addition to the constraints that can be converted to drag limits, the vehicle must also satisfy heat load constraints, which depend on the heat rate history over a given trajectory and cannot be plotted alongside the other constraints. The heat load, Q , can be approximated as:

$$Q \propto \int_{t_0}^{t_f} \sqrt{\rho} V^3 dt \quad (3)$$

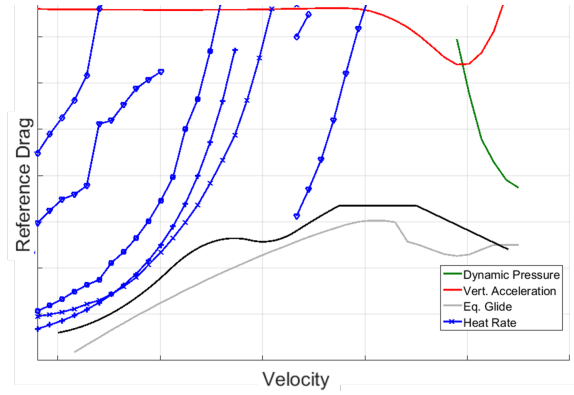


Fig. 2. Typical Constraints in Drag-Velocity Space

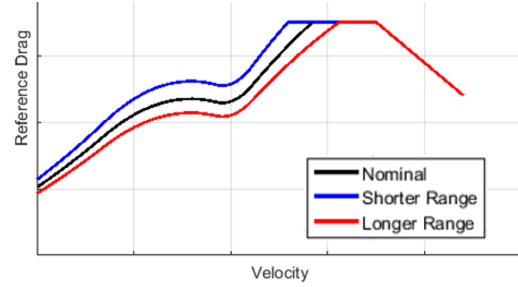


Fig. 3. Using D_1 to adjust profile range

Q can generally be minimized by decreasing flight time or by increasing drag during the initial part of the flight thereby decreasing it in later stages when air density is higher.

In general, a drag profile is designed for the nominal downrange to the runway expected after the deorbit burn. However, downrange varies under dispersed conditions, and aerodynamic and other modeling uncertainties can cause range errors to build up during a flight. As a result, the drag profile must be adjusted in real time to account for range errors. In the initial implementation of the Shuttle entry guidance, range error is removed by modifying only one drag profile parameter at a time. For any given parameter, the partial derivative of range with respect to the given parameter is used to linearize the system and compute new parameters used to define the new profile with the correct range. Only the drag profile segment currently being executed is modified, and all others are held constant, as seen in Figures 3 and 4. This forces the vehicle to follow the nominal profile as closely as possible, which ensures that the trajectory takes advantage of the large constraint margins under dispersed conditions that were prioritized when designing the profile.

The Shuttle algorithm modifies only one parameter when adjusting the drag profile to account for range errors during both the temperature control and equilibrium glide phase. By modifying D_1 , the reference curves for both phases are moved together, as seen in Figure 3. This method works well when the entry corridor is wide throughout the entire trajectory. However, when constraints are tight and the corridor is restricted, small range errors can easily cause constraint violations, as in Figure 5 with the turbulent flow

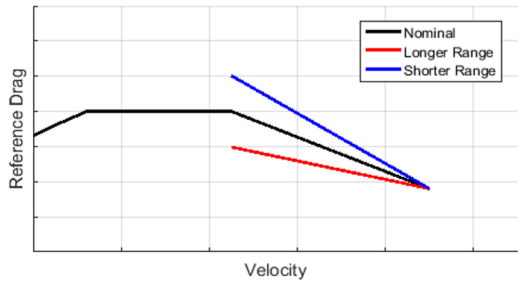


Fig. 4. Adjusting profile range during transition phase

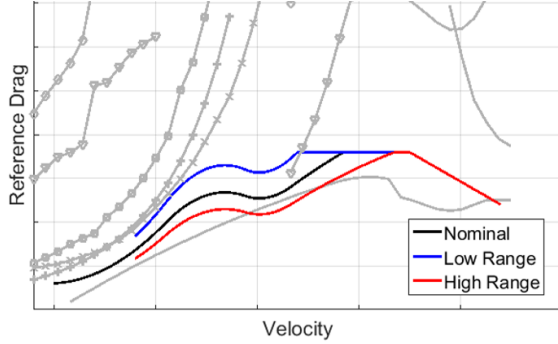


Fig. 5. When only D_1 is used, constraints are easily violated. The high and low range profiles start at lower velocities to demonstrate a profile being adjusted in flight.

transition heat rate constraint.

When making modifications to high TRL algorithms, maintaining the original structure is important for swiftly and reliably validating the code for flight. The proposed changes and additional profile modification parameters take advantage of the variables that are already used to define the drag profile and the methods used to compute range for each phase. Tighter constraints are likely to become more common as thermal protection systems are pushed to become lighter for overall vehicle weight reduction. As reusable orbiter designs are refined, methods that are robust to wide range dispersions while also leveraging flown Shuttle heritage algorithms will be necessary. The range allocation method presented in Section 3 proposes a modification that adds alternative methods for adjusting the drag profile. For a given range error during flight, adjusting multiple parameters allows the drag profile to remain sufficiently clear of constraints in known problematic regions while maintaining the algorithm's general structure.

Two specific cases are studied to motivate the utility and extent of this range allocator. The first is the case when the turbulent flow transition heat rate constraint is particularly restrictive, and the second is when tight heat load and heat rate constraints are both present.

III. PROPOSED RANGE ALLOCATOR DESIGN

The proposed range allocator design that follows is a new method for modifying reference drag profiles that improves the guidance algorithm's flexibility and helps to ensure that drag profiles generated on-line will still satisfy highly restrictive constraints.

A. Drag and Range Equations

The equation for range is simplified at high velocities using the assumption that $\gamma \ll 1$ deg, where γ is the flight path angle, as is seen in [1]. For cases when the small γ assumption is not valid, it is more accurate to use the assumption that $\cos \gamma \approx 1$ over $\sin \gamma \approx 0$, and therefore integration with respect to energy, E , is appropriate [1]:

$$R = - \int \frac{V \cos \gamma dV}{D(V) + g \sin \gamma} \approx - \int \frac{V dV}{D(V)} \quad (4)$$

$$R = - \int \frac{\cos \gamma dE}{D} \approx - \int \frac{dE}{D} \quad (5)$$

The calculation of range varies for each phase, since each uses a unique equation for reference drag, $D(V)$. The first phase, temperature control, is defined as a continuous series of quadratic curves. The coefficients that define these curves are found using a series of points that delineate the smooth quadratic spline, where the slope of the subsequent equilibrium glide phase is used to determine the boundary conditions of the spline. From V_0 to V_1 for spline i :

$$D_i(V) = D_1(c_{i1} + c_{i2}V + c_{i3}V^2) \quad (6)$$

The reference drag for the equilibrium glide phase is defined by Equation 7a, where V_s and D_1 are used to shape the profile. Equations 7b and 7c describe the reference drag profile during the constant drag and transition phases respectively, and Equation 7d is the energy equation used to schedule drag, where h is the altitude at V [1].

$$D(V) = D_1(1 - V^2/V_s^2)(1 - V_1^2/V_s^2)^{-1} \quad (7a)$$

$$D(V) = D_2 \quad (7b)$$

$$D(V) = D_4 + (D_4 - D_3)(E_4 - E_3)^{-1}(E(V) - E_4) \quad (7c)$$

$$E(V) = gh + \frac{V^2}{2} \quad (7d)$$

B. Range Equations

The range equation associated with the temperature control phase utilizes a quadrature rule to more easily calculate the range flown. In general, a given quadrature rule is defined by a set of points to evaluate along the interval, here (V_a, V_b, V_c) , as well as a set of constants to weight each evaluated point, (q_1, q_2, q_3) . Given $N+1$ knot locations, (v_i, d_i) , and quadratic coefficients for each spline, (c_{i1}, c_{i2}, c_{i3}) , the range can be approximated:

$$R = - \sum_{i=1}^N \int_{v_i}^{v_{i+1}} \frac{V dV}{D_i(V)} \quad (8)$$

$$R \approx - \sum_{i=1}^N (v_{i+1} - v_i) \left[q_1 \frac{V_a}{D(V_a)} + q_2 \frac{V_b}{D(V_b)} + q_3 \frac{V_c}{D(V_c)} \right] \quad (9)$$

The range equations for equilibrium glide and constant drag are significantly simpler, and can be evaluated directly. These are Equations 10 and 11 respectively.

$$R = \frac{V_s^2 - V_1^2}{2D_1} \log \left(\frac{D_2}{D_1} \right) \quad (10)$$

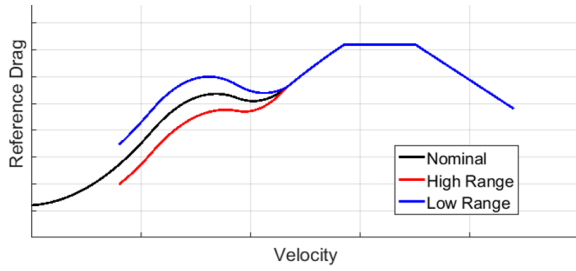


Fig. 6. Reference profiles with various k values.

$$R = \frac{V_2^2 - V_3^2}{2D_2} \quad (11)$$

C. Range Error Allocation Parameters

Three parameters have been selected for this allocator that allow for a wide range of profiles, D_1 , k , and V_s . Each parameter is assigned a weight that determines the proportion of range error, ΔR , that each parameter eliminates.

$$\Delta D_1 = (w_1 \Delta R)(dR/dD_1)^{-1} \quad (12)$$

$$\Delta k = (w_2 \Delta R)(dR/dk)^{-1} \quad (13)$$

$$\Delta V_s = (w_3 \Delta R)(dR/dV_s)^{-1} \quad (14)$$

$$w_1 + w_2 + w_3 = 1 \quad (15)$$

$$\Delta R = \frac{dR}{dD_1} \Delta D_1 + \frac{dR}{dk} \Delta k + \frac{dR}{dV_s} \Delta V_s \quad (16)$$

1) *Knob 1: Modifying D_1* : The point D_1 was used in the initial implementation of the Shuttle guidance algorithm, and was kept as a range error allocator parameter because it modifies the profile simply and has a large impact on profile range for a given small perturbation. Figure 3 demonstrates high and low range profiles that result from perturbing D_1 .

2) *Knob 2: Modifying k* : k defines the extremum of a quadratic curve that is defined by a vector of predetermined coefficients and is added to the set of quadratic splines in the temperature control phase. This augmented drag profile with the sum of two quadratic curves is

$$D'_i(V) = D_1(c_{i1} + c_{i2}V + c_{i3}V^2) + k(c_{q1} + c_{q2}V + c_{q3}V^2) \quad (17)$$

Figure 6 illustrates the effect of k on a given reference drag profile, where the modifying quadratic being scaled by k was set to 0 at the end of the temperature control phase. The simplicity of the calculation of dR/dk was an important factor when selected this parameter, particularly when compared to more obvious options such as using the value of a single spline knot as an allocator parameter.

Additionally, we considered the ability to tune the quadratic coefficients to respond to a variety of known problems. If the quadratic curve is set to 0 for a given velocity, changing k will not change the reference drag value at that location. This is ideal for locations where the size of the entry corridor is significantly reduced. Similarly, if the margin is known to be greater in a specific velocity region,

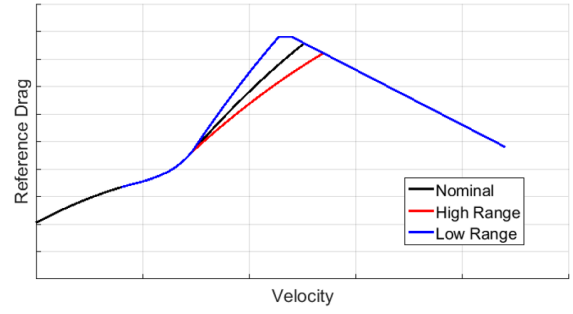


Fig. 7. Reference profiles with various V_s values

the magnitude of the quadratic curve should be greater in that region to take advantage of the wider constraints. This flexibility allows the reference drag profile to follow the shape of restrictive heat rate constraints that are typically most restrictive in up to two high velocity regions.

$$\frac{dR}{dk} = \sum_{i=1}^N -(v_{i+1} - v_i) \left[q_1 \frac{V_a(c_{q1} + c_{q2}V_a + c_{q3}V_a^2)}{D_1 D'_i(V_a)^2} + q_2 \frac{V_b(c_{q1} + c_{q2}V_b + c_{q3}V_b^2)}{D_1 D'_i(V_b)^2} + q_3 \frac{V_c(c_{q1} + c_{q2}V_c + c_{q3}V_c^2)}{D_1 D'_i(V_c)^2} \right] \quad (18)$$

3) *Knob 3: Modifying V_s* : The parameter V_s was chosen in part to provide multiple methods for modifying the equilibrium glide phase. By modifying V_s , it is possible to push the effects of a range error towards later in the trajectory, which is advantageous if constraints are particularly tight through the majority of the temperature control phase of the entry corridor. Figure 7 demonstrates the effects of changing V_s on a reference drag profile. The resulting equation used to update V_s at each time step is found in Equation 19.

$$\frac{dR}{dV_s} = \frac{V_s}{D_1} \log\left(\frac{D_2}{D_1}\right) + \frac{V_s}{D_2} \left(1 - \frac{D_2}{D_1}\right) \quad (19)$$

D. Design Discussion

This set of parameters was selected to span a much larger set of possible drag profiles, with likely limiting cases in mind. By choosing to use two parameters that are already used to define the profile, the structure of this algorithm continues to resemble the structure of the Shuttle heritage algorithm, preserving its simplicity. Furthermore, the selection of a quadratic curve that is added to the temperature control phase spline utilizes a significantly simpler dR/dk compared to other alternatives evaluated. Alternatives that were considered include modifying individual quadratic spline points, modifying individual cubic spline points, and modifying the magnitude of a quadratic that linearly scales the entire spline, as seen in Equation 20 for an individual spline, i . Although these alternatives could have provided more parameters to

modify in the allocator and more flexibility, the complexity of dR/dk in each of these outweighed potential benefits.

$$D_i(V) = D_1(c_{i1} + c_{i2}V + c_{i3}V^2)k(c_{q1} + c_{q2}V + c_{q3}V^2) \quad (20)$$

To ensure that all constraints are satisfied and that the profile slope is not too extreme for the vehicle to follow, a set of limits have been placed on the allocator parameters.

$$V_{s,min} < V_s < V_{s,max} \quad (21)$$

$$k_{min} < k < k_{max} \quad (22)$$

$$D_{min} < D_i(V) < D_{max} \quad (23)$$

When a parameter reaches a limit and is saturated, the allocator reapportions the weights, w , so that the weight of the saturated parameter is split among the other two in the same proportion as the remaining weights being augmented. Similarly, if two allocator parameters have been saturated, the remaining parameter will have weight $w = 1$ and will account for the entirety of the range error at that time step. Furthermore, this allocator is designed to work only during the temperature control phase. As a result, the allocator is restricted to a limited velocity range, where the lower limit is greater than V_1 to prevent large and potentially unachievable reference profile perturbations due to a small derivative, dR/dx for a given parameter x , and large range error, ΔR .

IV. ALLOCATOR PARAMETER SELECTION

The tunable variables available in the range error allocator are the points that define (c_{q1}, c_{q2}, c_{q3}) , and the weights (w_1, w_2, w_3) . A number of factors must be taken into account when selecting the range allocator parameters. First, the location of the most restrictive constraints will determine whether some locations of the drag profile should be restricted to be constant for the entire trajectory. The variance of the downrange distribution under dispersed conditions both after the deorbit burn and during flight informs how much range error the allocator can be expected to account for, and can be used to determine likely constraint violation locations. Each of the available parameters has a limited total range error it can account for during flight due both to the constraint locations and the design of the reference profile, and this should also be taken into account when selecting the weights, w . A recommended initial setting for (w_1, w_2, w_3) is found in Equations 24 - 26 where $\Delta R_{[]}$ is the total range span that results from pushing the given parameter to its minimum and maximum allowable values. This initial setting will allow the parameters to move together without encountering a limit after accounting for just a small range error.

$$w_1 = \Delta R_{D_1} / (\Delta R_{D_1} + \Delta R_k + \Delta R_{V_s}) \quad (24)$$

$$w_2 = (\Delta R_k) / (\Delta R_{D_1} + \Delta R_k + \Delta R_{V_s}) \quad (25)$$

$$w_3 = (\Delta R_{V_s}) / (\Delta R_{D_1} + \Delta R_k + \Delta R_{V_s}) \quad (26)$$

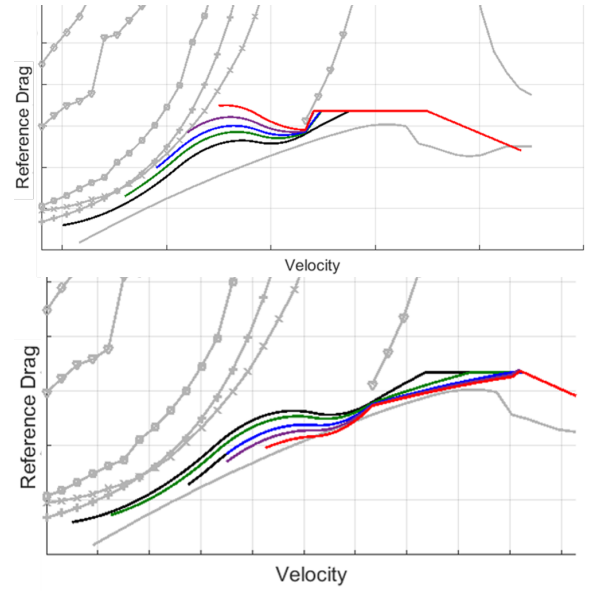


Fig. 8. Example profiles for range errors with full set of allocator parameters (Top - Short Profiles, Bottom - Long Profiles). By using all 3 allocator parameters to account for range error, the profiles satisfy all constraints.

Finally, the consequences of violating each individual constraint, results under dispersed conditions, and the vehicle's ability to track reference drag commands should be considered in selecting weights.

V. RESULTS

The proposed range allocator can be used to satisfy a number of extremely restrictive constraints. In Figure 8, the profiles satisfy both the set of high velocity heat rate constraints (left 5 constraints) and turbulent flow transition heat rate constraint. These profiles use $w_1 = 0.1$, $w_2 = 0.85$, and $w_3 = 0.05$. The success of this example is clear given that constraints that would have otherwise been violated (as seen in Figure 5) can be satisfied while still accounting for the same range error.

This range allocator can also be used to satisfy restrictive heat load constraints. In general, heat load can be mitigated by maintaining high drag in the high velocity part of the trajectory and decreasing drag later in the trajectory. Decreasing drag across the entire profile tends to increase range, which increases flight time and therefore heat load, while increasing drag across the entire profile tends to increase the heat rate, which also results in a higher heat load. To demonstrate the value of this allocator in satisfying this constraint, two sets of parameter weights are examined when the vehicle state after deorbit is one that stresses the heat load constraint. Typically, the heat load stressing case involves an initial state that has a longer than nominal downrange as well as a steeper flight path angle, while the opposing heat rate stressing case involves an initial state that has a shorter than nominal downrange and shallower flight path angle.

The first set of allocator weights used are $w_1 = 1.0$, $w_2 = 0.0$, and $w_3 = 0.0$, which only uses D_1 to account for

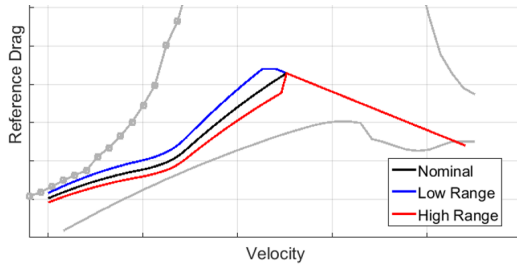


Fig. 9. Example profiles using first set of weights, when only the D_1 parameter is being modified. The heat load stressing case will likely violate heat load constraints because drag is decreased at high velocity.

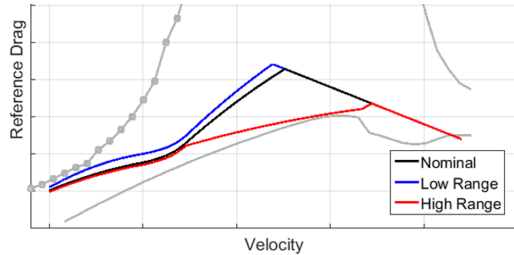


Fig. 10. Example profiles using the second set of weights, (both D_1 and V_s are being modified). The heat load stressing case will likely have a lower Q because drag remains at its nominal value at high velocity.

range error, and is equivalent to the original algorithm implementation. When this allocator encounters a heat load stressing case, the profile will be shifted down across both the temperature control and equilibrium glide phases. However, this will result in lower drag at high velocity, which will likely increase the heat load (See Figure 9). The second set of allocator weights used are $w_1 = 0.3$, $w_2 = 0.0$, $w_3 = 0.7$, which uses both D_1 and V_s to account for range error. Because the equilibrium glide phase is modified independently of the temperature control phase, the reference drag at high velocity remains largely undisturbed. This is expected to result in a lower heat load compared to the first set of weights. Example reference profiles for this second set of weights can be found in Figure 10.

Both sets of weights were implemented and used to run a vehicle simulation with heat load stressing initial conditions. The resulting reference profiles in Figure 11 are similar to those we would expect based on Figures 9 and 10. While the initial reference profile defined before flight is the same for both the (D_1) case and the (D_1, V_s) case, the different weights result in different reference profiles in flight once the vehicle encounters a large range error upon deorbit. In the allocator heat load stressing case, the heat load was decreased in many areas of concern, in some locations by up to 1.25%. By implementing additional parameters to account for range error, the heat load was decreased under the most stressing initial conditions without requiring large changes to the structure of the algorithm.

VI. CONCLUSIONS

The design of the proposed range allocator includes multiple parameters that can be modified on line to account for

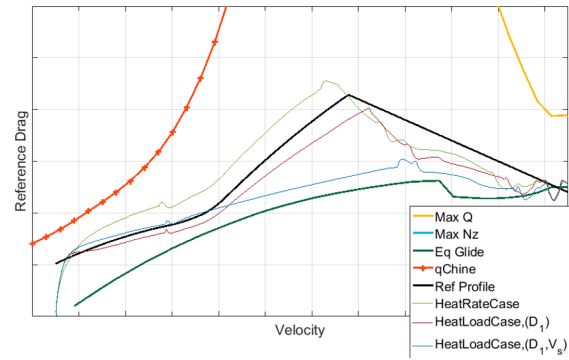


Fig. 11. Example profiles for long range errors with full set of allocator parameters. By using all 3 allocator parameters to account for range error, the profiles satisfy all constraints.

range error during flight. The design of the quadratic curve associated with k in addition to the selection of weights used to allocate range error to each parameter results in a more flexible guidance algorithm. Notably, the range allocator presented here also preserves both the way the drag profile is defined as well as the overall structure of the algorithm.

Two specific sets of constraints are examined using the proposed range allocator. The first includes high velocity heat rate and turbulent flow transition heat rate constraints. With the use of the range allocator, all constraints can be satisfied. The second includes a requirement to minimize heat load. Using the range allocator, heat load is decreased in known problem areas. Future work might include optimizing the weights off line using heat load, reference profile slope, or other measures of vehicle performance, and modifying the algorithm to be memoryless with respect to range error. Furthermore, scheduling the weights based on velocity or adding D_2 as an additional parameter may provide an additional degree of flexibility that allows more range to be added to parameters that affect later portions of the trajectory as the vehicle progresses along its trajectory.

REFERENCES

- [1] J. C. Harpold and C. A. Graves Jr, "Shuttle entry guidance," in *American Astronautical Society, Anniversary Conference, 25th, Houston, Tex., Oct. 30-Nov. 2, 1978*, 35 p., vol. 1, 1978.
- [2] J. M. Hanson, D. J. Coughlin, G. A. Dukeman, J. A. Mulqueen, and J. W. McCarter, "Ascent, transition, entry, and abort guidance algorithm design for the x-33 vehicle," *AIAA paper*, vol. 98, p. 4409, 1998.
- [3] P. Lu and J. M. Hanson, "Entry guidance for the x-33 vehicle," *Journal of Spacecraft and Rockets*, vol. 35, no. 3, pp. 342–349, 1998.
- [4] P. Lu, "Entry guidance and trajectory control for reusable launch vehicle," *Journal of Guidance, Control, and Dynamics*, vol. 20, no. 1, pp. 143–149, 1997.
- [5] G. A. Dukeman, "Profile-following entry guidance using linear quadratic regulator theory," *AIAA paper*, vol. 4457, pp. 5–8, 2002.
- [6] J. D. Schierman, D. G. Ward, J. R. Hull, N. Gandhi, M. W. Oppenheimer, and D. B. Doman, "Integrated adaptive guidance and control for re-entry vehicles with flight-test results," *Journal of Guidance Control and Dynamics*, vol. 27, pp. 975–988, 2004.
- [7] W. Grimm, J. van der Meulen, and A. Roenneke, "Optimal update scheme for drag reference profiles in an entry guidance," *Journal of guidance, control, and dynamics*, vol. 26, no. 5, 2003.
- [8] K. Mease, D. Chen, S. Tandon, D. Young, and S. Kim, "A three-dimensional predictive entry guidance approach," in *AIAA Guidance, Navigation, and Control Conference and Exhibit*, 2000, p. 3959.